The Interpretation of Separation Mechanism of Ridge-Cut Explosive Bolt Using Software Simulation Program

Y. J. Lee and D. J. Kim *
Agency for Defense and Development, and Hanwha Corporation *
TEDC-4-7, ADD, Yusung P.O.B 35-5, Taejeon, Korea
yeungjolee@nate.com

Keywords: Explosive Bolt, Separation Mechanism, Failure Mode, AUTODYN Program, Design Factor, 3-D Modeling, Interpretation Processor

Abstract

The present work have been developed the interpretation processor including the behavior of material failure and the separation phenomena under transient dynamic loading (the operation of explosive bolt) using AUTODYN V4.3, SoildWork 2003 and TrueGrid V2.1 programs. It has been demonstrated that the interpretation in ridge-cut explosive bolt under dynamic loading condition should be necessary to the appropriate failure model and the basic stress of bolt failure is the principal stress. The use of this interpretation processor developing the present work could be extensively helped to design the shape and the amount of explosives in the explosive bolt having a complex geometry. It is also proved that the interpretation processor approach is an accurate and effective analysis technique to evaluate the separation mechanism in explosive bolts.

1. Introduction

Explosive bolts are reliable and efficient mechanical fastening devices having the special feature of a built-in release. They are ideally used in space shuttle, missile, aircraft and underwater vehicle systems, for example for launcher operation, stage separation, release of external tanks, thrust termination and many other applications[1].

Numerous different shapes and sizes of explosive bolts have been thus far developed for a great variety of applications. Very careful consideration[2] is required the design factors such as firing characteristics, shape and size, kind of explosive material, quantity of explosive material and environmental conditions under restraint during the time of design of explosive bolt. The most suitable design of explosive bolt is necessary for separation characteristics without fragmentation and minimum pyro-shock during the operation of the explosive bolt. It is recommended the optimum of all design factors rather than the individual design factor because of the systematically influence of the individual design factor. It is required a number of time and sample to select the optimum design factor by the actual experimental method[3-4] including design, manufacture, test and data-collecting in turn. So far a number of data have been accumulated concerning the separation mechanism of the explosive bolts developing conventional method.

Using the actual experimental data and the interpretation processor data, the present study develops the interpretation processor including the behavior of material and separation phenomenon under transient dynamic loading (the operation of explosive bolt). The programs used the present work is SoildWorks 2003, TrueGrid V2.1, Tgio.exe.and AUTODYN V4.3. It is also proved that the interpretation processor approach is an accurate and effective analysis technique. The interpretation processor could be able to make the design of explosive bolt without actual production, and to reduce especially the developing time and money.

A schematic diagram of interpretation used the present work is shown in Fig. 1.

2. Conception of Design and Shape in the Ridge-Cut Explosive Bolt

Ridge-cut explosive blot is consisted of initiator, sleeve, main bolt body, cartridge assembly, explosive as shown in Fig. 2. Explosive is not expressed in 3-dimension model. In the present work, seal not effecting strength is excluded to numerical method, and restriction body for separation time, which is the section applied boundary condition and is able to directly influence on the result of numerical method, is included numerical method to compare the correlation between the numerical results and the actual experimental results. Among lead azide (LA), PETN and RDX, LA does not include numerical method because of not a great influence on bolt body. The initiation of explosive assumes the contact plane between the PETN and the RDX. Figure 3 shows the mechanism of ridge-cut and the application of the ridge-cut explosive bolt

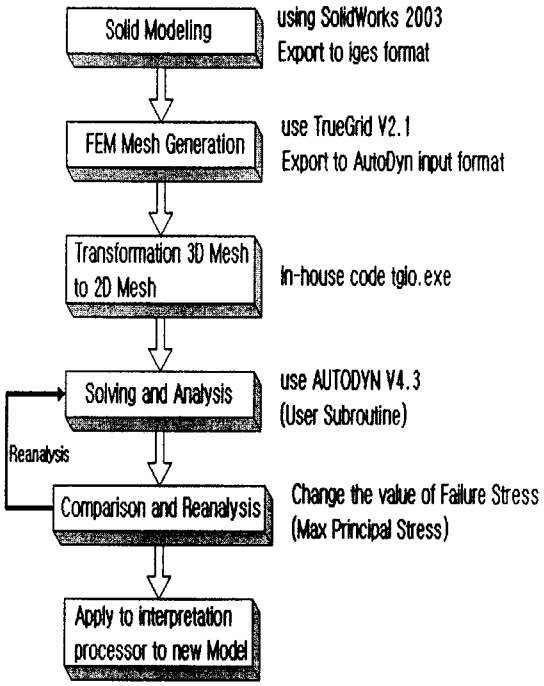

Fig.1. A schematic diagram of Interpretation

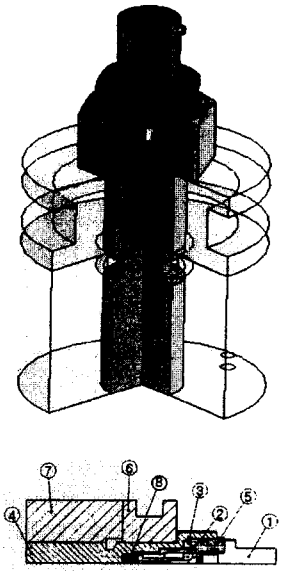

1: Initiator
2: Sleeve
3: Seal
4: Bolt Body
5: Cartridge Assembly
6,7: Measuring Body of Separation Test
8: Explosive

Fig. 2. Shape and Model of Ridge-Cut Explosive Bolt

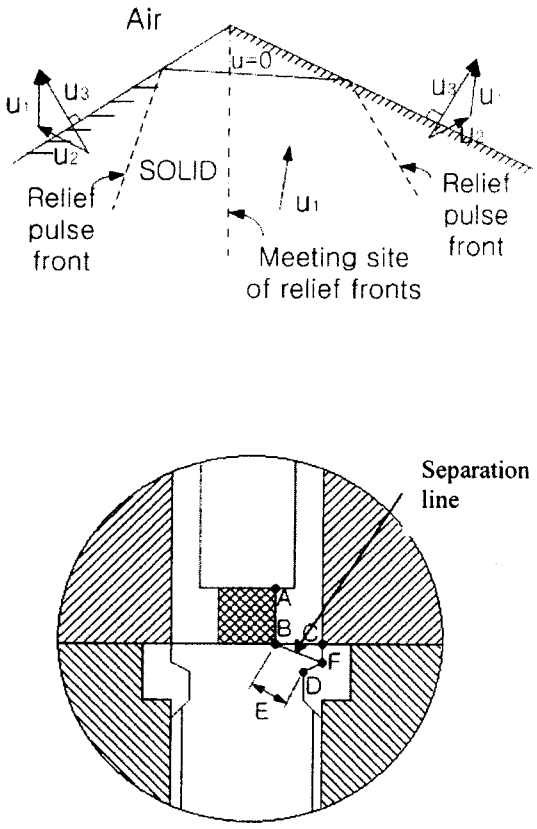

Fig. 3. Mechanism of Ridge-Cut By Meeting of Relief Fronts and Application of Ridge-Cut Explosive Bolt

Detonation high explosives against one side of a steel body that presents sharp ridges at the other side gives rise to a type of fracture that is not intelligible on the basis of the classic theories of fractures and of elastic waves[5]. The-mechanism of ridge-cut[6] is quite clear if the course of the relief pluses along the metal boundary on each side of a sharp ridge is followed as shown in Fig. 3. As the incident shock pulse progresses towards the ridge itself, the relief pulses delimit two high velocity regions on either side of the latter, moving in different directions. The boundary conditions indicate further that these regions are not subjected to any stress at all. At the instant in which the incident shock pulse vanishes at the ridge, the high velocity zones achieve a common boundary along the meeting site of the relief pulses, which is located along a bisector of the ridge angle. The particles located on either side of this common boundary part company instantly by virtue of their individual kinetic energies without benefit of any tensile stresses, which may be induced later in the metal as the front of the relief pulses flatten out. No conceivable stress can possibly exist at the sharp ridge itself, where the cut originates. Separation of ridge-cut explosive bolt occurs along BF line originated the mechanism of ridge-cut as shown in Fig. 3.

3. Interpretation Model of Explosive Bolt

3.1 Model of Shape and Numerical Method

Figures 4-7 show the modeling of shape and finite element in the four different models used the present interpretation. Creating a model of shape is used SolidWorks and whole assembly is made from a model of explosive bolt consists of individual item. Figures 4-7 appear the assembly cutting one quarter to rotation direction and they are also represented with the finite element method conducting the TrueGrid program of finite element method. The TrueGrid implements the powerful projection method and generates a mesh by projection a block mesh of our choice of refinement onto any geometry. The projection to surface takes advantage of the differentiability of the surface. Each surface is approximated by an array of polygons. These polygons are used to display the surface. When a node is to be projected to such a surface, the initial 3D coordinates of the node are used to search the coordinates of the surface approximation. Each surface has a complex data structure to optimize this search. The point on the surface approximation, being closest to the node is then mapped back to the parametric coordinates of the surface. The TrueGride information should be informed to the AUTODYN using structured mesh method. Not all cells defined the computational space need to be defined in physical space. This allows complicated geometry to be meshed. To improve efficiency of time step, "unused cell" technique is used in AUTODYN. Figures 4 and 6 are represented models when "unused cell" is not applied, and Figures 5 and 7 show models using "unused cell". In the case of the explosive bolt composed several items, different subgrids may interact with each other via "external Lagrange-Lagrange interaction" in AUTODYN. The external gap size is 0.02 mm.

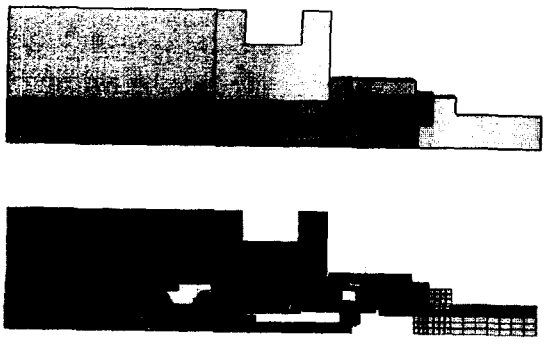

Fig. 4. Model of Shape and Finite Element Method in Model #1

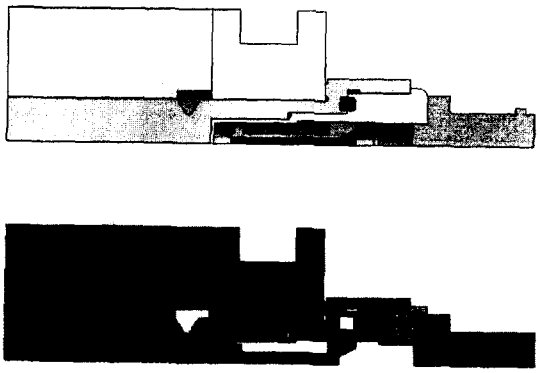

Fig. 5. Model of Shape and Finite Element Method in Model #2

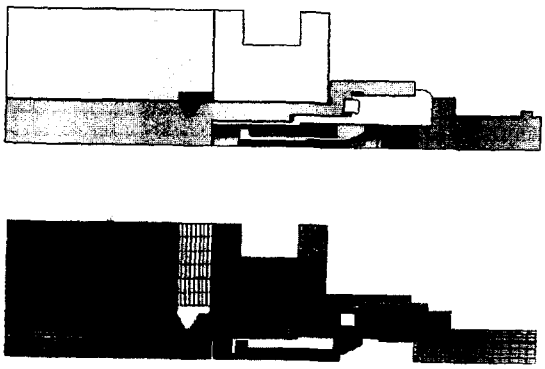

Fig. 6. Model of Shape and Finite Element Method in Model #3

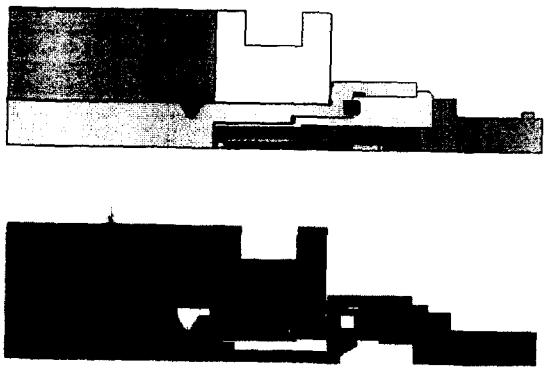

Fig. 7. Model of Shape and Finite Element Method in Model #4

Table 1 is represented the characteristics and applications of models.

Table 1 The Characteristics and Applications of Models.

		Model #1	Model #2	Model #3	Model #4
Cartridge Model No.		1	2	←	←
Shape of Explosive	kind	RDX			
	Height	5.2mm	3.17mm	4.0mm	1.67mm
	Radius	3.0	3.75	←	←
Ridge Angle		120°	←	←	←
Test Results		Always separation	Separation or non separation	Always separation	Always non separation
use		Demonstrate Interpretation processor	Estimate Failure Stress		

3.2 Materials Models

Table 2 provides materials modes used in the interpretation of the explosive bolt. AUTODYN is generally used to analyze the behavior of materials under transient dynamic loading. To describe in details the behavior of materials and the separation phenomena, thus, equation of art (EOS), strength model and failure model concerning materials of ridge-cut explosive bolt should be provided.

Table 2. Materials Models

	EOS Model	Strength Model	Failure Model	Erosion Model
PETN	JWL	Hydro	None	Instantaneous Geometric strain
RDX	↑	↑	↑	↑
17-4PH	Shock	Johnson-Cook	Principal Stress	↑

JWL(Johnson-Wilkins-Lee) EOS used to model the rapid expansion of high detonation products and is empirical. The pressure for the expanding gas is given by

$$p = C_1(1-\frac{\omega}{r_1 v})e^{-r_1 v} + C_2(1-\frac{\omega}{r_2 v})e^{-r_1 v} + \frac{\omega e}{v} \quad \text{-(1)}$$

Where C1, C2, r1, r2, w are empirically derived constants and v = density, e = specific internal energy. In the case of 17-4PH, the Mie-Gruneisen form of EOS can be written as

$$p = p_r(v) + \frac{\Gamma(v)}{v}[e - e_r(v)] \quad \text{-(2)}$$

Where the subscript r denotes the values of pressure and internal energy along some known reference curve and F is a function of density only and is known as the Gruneisen Gamma. This form can be solved simultaneously with the energy the equation without need for any iteration. Also 17-4PH has a higher ultimate tensile stress than that of other metals, Johnson-Cook model, which is a purely phenomenological model, with data found from experimentent (Spilt Hopkinson Bar). The yield stress is given by

$$Y = [A + B\varepsilon_p^n][1 + c\log\varepsilon_p^*][1 - T_H^m] \quad \text{-(3)}$$

ε_p = effective plastic strain

ε_p^* = normalized effective plastic strain

$T_H = (T - T_{room})/(T_{melt} - T_{room})$, homologous temperature

Where, Y is yield stress and is dependant upon temperature. To apply Johnson-Cook model, A, B, c, m, n and T_H should be obtained from the experimental condition and materials. Most materials can only withstand relatively small tensile stresses and/or strains before they fail. Several criteria exist in AUTODYN to determine the onset of failure. Failure model of 17-4PH is based on principal failure model, which is occurred failure when maximum principal stress (or strain) exceeds failure stress (or strain) or when maximum shear stress (or strain) exceeds failure stress (or strain). On initiation of failure by a failure mechanism, the stress deviators are set to zero (i.e. the material is hydrodynamic) and only to positive pressures may be sustained. If the pressure is negative it will be reset to zero. Murr and Kuhlmann –Wilsdorf have demonstrated[5] the hardening of metals and alloys by shock loading to be at least a few times greater than the hardening that would normally result from the same amount of deformation (equivalent strain) in a tensile test. This is one of the unique features of shock deformation recognized in the early experiments of Murr and others[5].

Failure stress resulted from a tensile test is not suitable to directly apply to the present failure model and also failure stress of high strain rate (10^{-6}/sec) could not be obtained from actually experimental test. The present work decides to the failure stress of 17-4PH to evaluate and compare the failure stress of the actual experimental work with the interpretation work. As shown in table 1, the failure stresses of three different types apply to numerical method. Table 3and 4 are represented in details the characteristics of explosives and 17-4PH materials necessary to the present interpretation.

Table 3 The Characteristics of Explosives

성수 [단위]	C_1 [kPa]	C_2 [kPa]	R_1	R_2	ω	ρ [g/cm3]	V_{cj} [m/sec]	P_{cj} [kPa]	E_0/vol [kJ/m3]	Erosion strain
PETN 1.20	5.731E8	2.016E7	6.0	1.8	0.260	1.20	6.589E3	1.57E7	7.19E6	2
RDX 1.16	6.113E8	1.065E7	4.4	1.2	0.258	1.16	6.653E3	1.56E6	6.30E6	2

Table 4 The Characteristics of 17-4PH

상수 [단위]	A [kPa]	B [kPa]	n	C	m	T_m [K]	ρ [g/cm3]	Γ	G [kPa]	ν	Erosion strain
17-4PH	1.47E6	4.47	0.18	0.012	1	1763	7.86	2.17	2.0	0.272	3

3.3 Boundary Conditions

In addition to initial conditions, boundary conditions are required to fully specify problem. Due to the local nature of many applications in AUTODYN, it is often only necessary to model a part of the entire geometry (i.e. the effect of the remaining geometry is represented by boundary conditions). Boundary conditions of the present work should be included stress, velocity, point and force boundary conditions. ALE (Arbitrary Lagrange Euler) solver, which material interfaces are Lagrange and interior cells may be Lagrange, Euler or any other motion constraint, is used in the present work. The ALE computation cycle is identical to that for Lagrange with an additional rezoning step for interior nodes. Interior nodes are zoned according to specified motion constraints and the solution is mapped onto the new grid. The warp-up cycle of computation is established 30,000 cycles.

The regions excluded different regions (subgrids) interacted with each other are calculated "Lagarnge-Lagrange Contact". Figure 8 shows the subgrid points of joint boundary conditions in the explosive bolt and points of joint (dark node) can be specified for each subgrid to subgrid join.

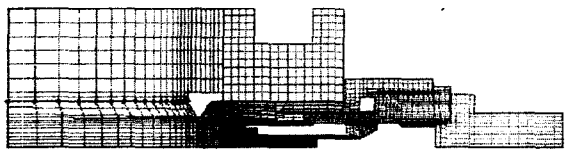

Fig. 8. Joint Boundary Conditions

Figure 9 is represented the velocity boundary conditions established constraint conditions during the operation explosive bolt. The red node in body of measuring separation time is fixed zero of velocity of X, Y directions.

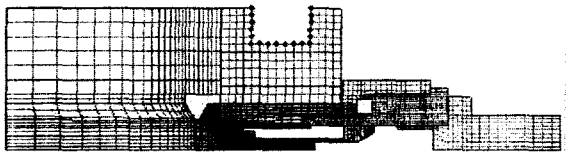

Fig. 9. Velocity Boundary Conditions

Normally, detonation paths are computed by calculating a straight line from the detonation node to each cell center. However, the indirect path option is used in the present work. Indirect option paths are computed by finding the shortest path obtained by following straight lines segments connecting centers of cells containing explosives. The beginning time of detonation (0 sec.) is established to the start time of the interpretation program. The RDX and PETN explosives are modeled in same subgrid.

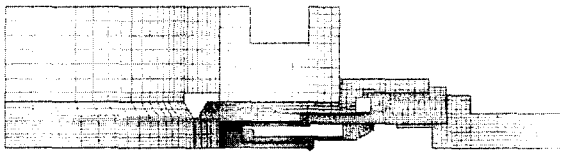

Fig. 10. Detonation Point

4. Numerical Methods

Finite element method used in the present work is firstly conducted to calculate the failure stress of the explosive bolt throughout models 2-4 and is secondary established whether the failure stress calculated to the first step accords with the actual experimental work of model 1 or not.

4.1 Calculation of Failure Stress

Two different methods are calculated to estimate the failure stress from the actual experimental data and the numerical method data. Whether failure model applies to or not.

4. 1. 1 Non Application of Failure Model Method

In the case of non application of failure model method, 72 gauge points is set up the place between the explosives and the region ridge-cut to evaluate the principal stresses in the section of sleeve and bolt body as shown in Fig. 11. The gauge points used is Lagrange type.

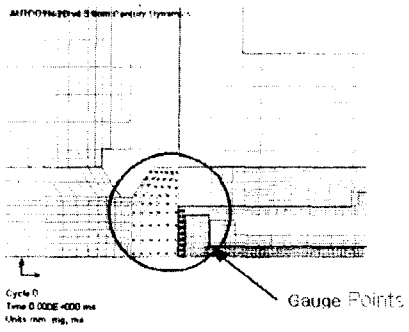

Fig. 11. Gauge Points

Figures 12-14 show the changes of the principal stress with the operation time resulting from the stress condition of gauge points. The present work is considered not the location of the principal stress but the value of the principal stress during the calculation. The results have been calculated that the value of the principal stress is very high compare to that of actual. Although the value of the principal stress depending

on models is a little difference, the value is 4-28 times of the failure stress (1.5E6 kPa) resulting from static condition. Actually, comparing the calculation of the principal stress with each model, model #3 is always founded the failure phenomena and model #4 is never detected the failure mode in the experimental results. It is thus demonstrated that non application of failure model method can not be carried out to analyze the behavior of separation phenomena in case of the ridge-cut explosive bolt used present study, which the deformation of material is too large to cause the failure of material under transient dynamic loading. If the application of a proper failure model is not applied to the calculation, the distribution and value of the principal stress resulting from the calculation could not be trusted.

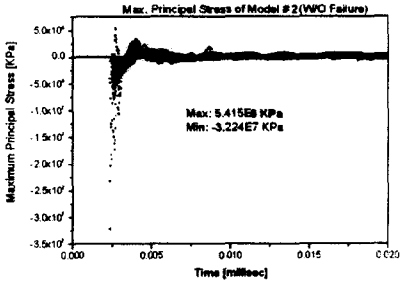

Fig. 12. The Changes of the Principal Stress with the operation Time in Model #2

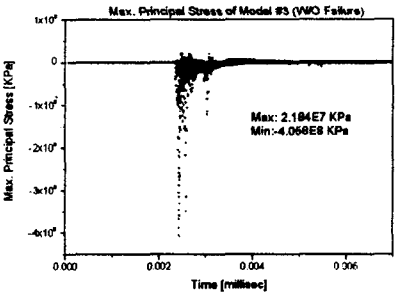

Fig. 13. The Changes of the Principal Stress with the operation Time in Model #3

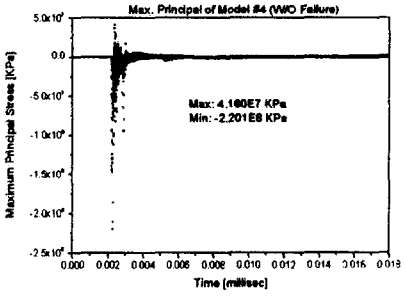

Fig. 14. The Changes of the Principal Stress with the operation Time in Model #4

4. 1. 2 Application of Failure Model Method

In case of application of failure model method, gauge points shown in Fig. 11 is not needed the calculation and it has been only focused to evaluate the coincidence of results from the actual experimenting and the calculation. The failure stress, i. e. static tensile stress (1.5E6kPa) is gradually increased to compare to that of the experimental work in the application of failure model method. When failure stress is approximately 2 times of static tensile stress (2.8~3.0 E6 kPa), it is good correlated the actual experimental results and the calculation. Figures 15(a) and (b) are represented the beginning time of the failure (3.494 μsec) and finishing time of calculation in failure mode, respectively. The initiation of failure is occurred to near the region of ridge-cut, but the result is not originally designed in the failure mode. The initial design of failure is the region of upper direction of the present observation. It is considered that the precise failure of ridge-cut is necessary to change the increase of the explosive diameter. After calculation, the subgrid of failure mode is detected to only one element in the region of middle. So it is not confirmed whether model #2 is occurred always a failure or not. Figure 16 shows the distribution of pressure at the initiation of failure. It is appeared to affect the tensile stress in the region between the ridge and the corner of sleeve.

Figures 17(a) and (b) show the failure mode in model #3. The initiation of failure is quietly similar to that of model #2 (3.474 μsec) and the region of failure is also same one. After calculation, it is informed that the region of failure is larger compare to that of model #2. Figure 18 shows the distribution of pressure at the initiation of failure as same as model #2. Figures 19(a) and (b) show the failure mode in model #4. The initiation of failure (4.112 μsec) is too late compare to that of model #2 and model #3. The region of failure is quietly different from that of model #2 and model #3, the reason is caused from using small explosive to make the failure of ridge-cut. It is also demonstrated in Fig. 20 that the distribution of tensile stress appears to be small band comparing that model #3.

(a) Beginning Time of Failure Mode

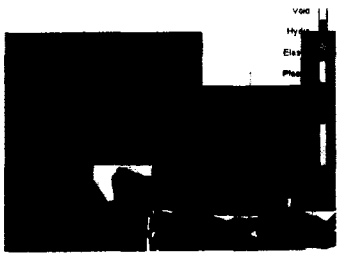

(b) Finishing Time of Failure Mode

Fig. 15. Failure Mode of Model #2

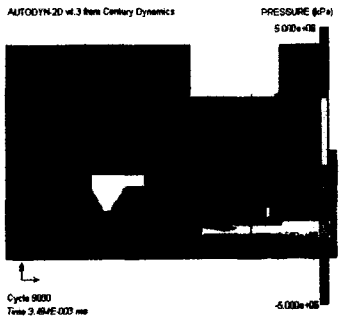

Fig. 16. The Distribution of Pressure at the Initiation of Failure in Model #2

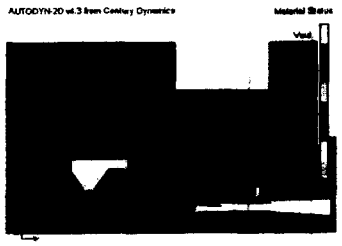

(a) Beginning Time of Failure

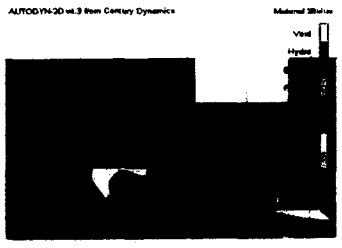

(b) Finishing Time of Failure Mode

Fig. 17. Failure Mode of Model #3

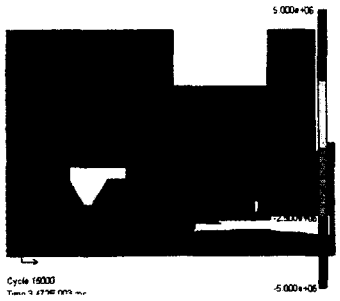

Fig. 18. The Distribution of Pressure at the Initiation of Failure in Model #3

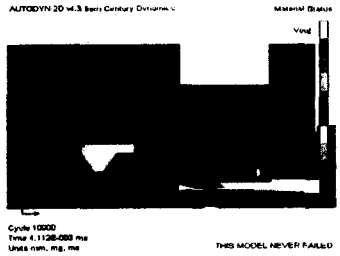

(a) Beginning Time of Failure

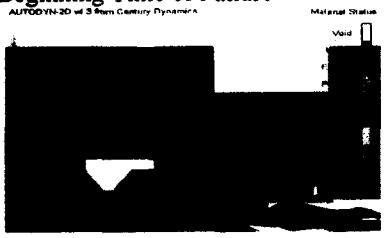

(b) Finishing Time of Failure Mode

Fig. 19. Failure Mode of Model #4

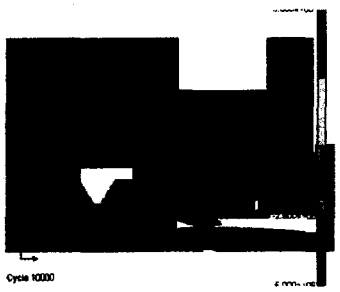

Fig. 20. The Distribution of Pressure at the Initiation of Failure in Model #4

4. 1. 3. Comparison of the Experiments with the Calculation

Figures 23(b)-(e) show the shape of the ridge-cut explosive bolt used the present model #2 - #4 after separation test. It is clearly shown in the application failure model method that the result of calculation is agreed with that of the separation test experiments.

5. Application of Other Models with Failure Model

Some difference Model #1 having the changes of the amount of explosive and the shape of design is applied to the failure stress calculated in the application of failure model method. Figures 21(a) and (b) show the failure mode in model #1. The beginning time of failure (3.474 μsec) is similar to that of model #2 and #3, but the region of the failure occurrence is quietly different from that of model #2 and #3. In the model #1, the initiation of failure is occurred firstly the contact plane of the bolt body and the restriction body of separation test, and after that the failure progress the region of undercut opposite to the ridge, the center region of bolt body, the region of the restriction body of separation test, finally the line (region) between the ridge and the sleeve. The failure mode in model #1 is informed that the line of failure is apart from ridge-cut section and the conception of original design; that is not completely ridge-cut mechanism.

After the calculation finishes, the failure mode in model #1, the region of failure is quite large and several numbers of failures are occurred. It would be thus predicted the occurrence of fragments after the actual operation of explosive bolt. The reason is come from the large amount of explosive, so the changes of shape and the amount of explosive should be needed. In the case of model #1, the actual experimental result is similar to that of the calculation as shown in Fig, 23(a). It can be easily known in Figure 22 that the distribution of pressure at the initiation of failure is not normal comparing these of model #2 and #3.

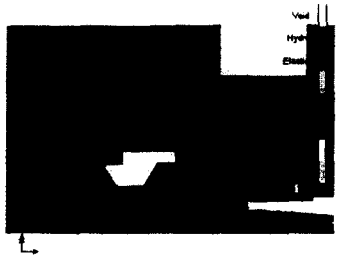

(a) Beginning Time of Failure

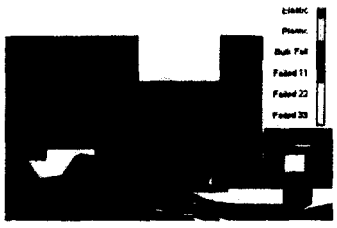

(b) Finishing Time of Failure Mode

Fig. 21. Failure Mode in Model #1

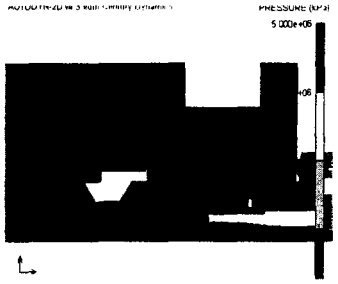

Fig. 22. The Distribution of Pressure at the Initiation of Failure in Model #1

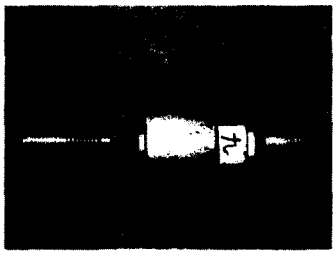

(a) The Shape of Explosive Bolt After Separation Test in Model #1

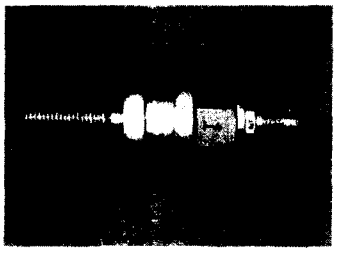

(b) The Shape of Explosive Bolt After Separation Test in Model #2 (Non separation)

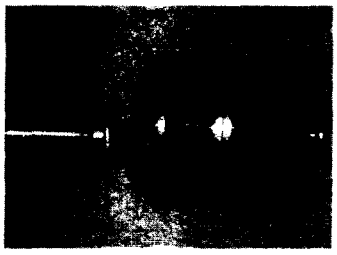

(c) The Shape of Explosive Bolt After Separation Test in Model #2

(d) The Shape of Explosive Bolt After Separation Test in Model #3

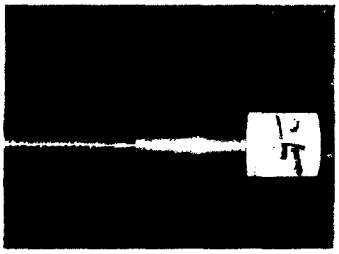

(e) The Shape of Explosive Bolt After Separation Test in Model #4 (Non separation)

Fig. 23. The Shape of Explosive Bolt After Separation Test in Model #1-#4

Other explosive bolts having the changes of the explosive height are calculated with the same failure stress used in model #2 and #3. The height and the amount of explosive used the actual experimental test is changed such as 1.5mm(85mg), 1.8mm(95mg), 2.0mm(102mg), 2.5mm(134mg), 3.0mm(166mg), 3.5mm(185mg) and 4.0mm(210mg). Figures 24-30 show the failure mode with the changes of explosive height at the beginning time (0 cycle, 0 sec.) and the finishing failure time (12,000cycle, 4.3 μsec). The initiation of failure in all samples is approximately 3.2 μsec (9000 cycle) expect the sample of 1.5 mm and the failure in all samples is completely occurred at the 4.3 μsec expect the samples of 1.5 mm and 1.8 mm. The sample of 1.5 mm in Fig. 32 (a) does not detected the progress of failure and the sample of 1.8 mm in Fig. 32 (b) can be not informed the complete progress of failure. Although there are including the changes of the location and the progress of failure, the samples of 2.0, 2.5, 3.0, 3.5, 4.0 mm are surely identified the completetion of the failure as shown in Figs 32 (c) - (g). The present result is quietly similar to that of the actual experimental one, the samples of 1.5 mm and 1.8 mm are not separated after separation test under unrestraint condition, but the samples of 2.0, 2.5, 3.0, 3.5, 4.0 mm are always separated similar to these of the calculation. All samples separated in the actual experimental tests have a clear and sharp separation plane like a knife. These results show that the failure mode in the samples of 2.0, 2.5, 3.0, 3.5, 4.0 mm are more completely happened than those of models #2 and #3, that is a perfect ridge-cut failure. Also we can see in the present work that the morphologies of separation plane are similar to that of samples having complete separation failure mode; that is, the morphology of 2.0 mm is similar to one of 4.0 mm. Through the present work, the interpretation processor developed using AUTODYN program including the behavior of materials failure and the separation phenomena under transient dynamic loading could be able to make the design of explosive bolt without actual production, and to reduce especially the developing time and money.

(a) 0 cycle

(b) 12000 cycles

Fig. 24. Failure Mode in 1.5 mm

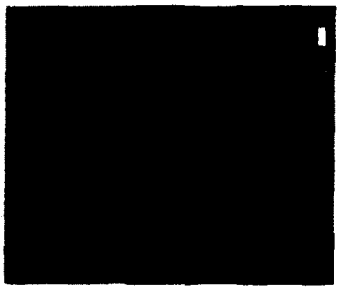

(a) 0 cycle

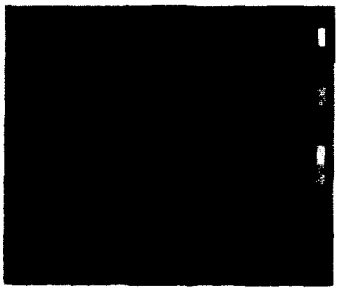

(b) 12000 cycles

Fig. 25. Failure Mode in 1.8 mm

(a) 0 cycle

(b) 12000 cycles

Fig. 26. Failure Mode in 2.0 mm

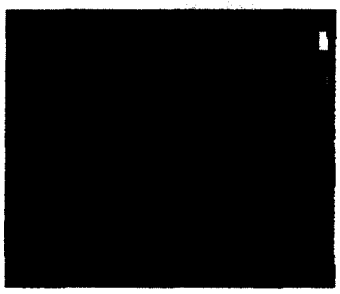

(a) 0 cycle

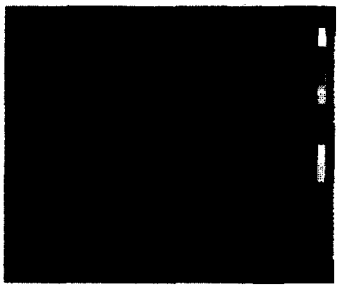

(b) 12000 cycles

Fig. 27. Failure Mode in 2.5 mm

(a) 0 cycle

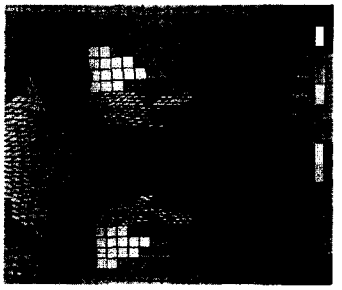

(b) 12000 cycles

Fig. 28. Failure Mode in 3.0 mm

(a) 0 cycle

(b) 12000 cycles

Fig. 29. Failure Mode in 3.5 mm

(a) 0 cycle

(b) 12000 cycles

Fig. 30. Failure Mode in 4.0 mm

(a) The shape of 1.5 mm Sample After Separation Test

(b) The shape of 1.8 mm Sample After Separation Test

(c) The shape of 2.0 mm Sample After Separation Test

(d) The shape of 2.5 mm Sample After Separation Test

(e) The shape of 3.0 mm Sample After Separation Test

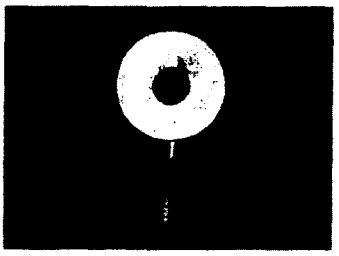

(f) The shape of 3.5 mm Sample After Separation Test

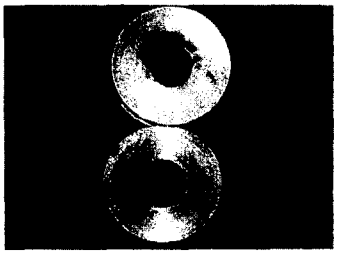

(g) The shape of 4.0 mm Sample After Separation Test

Fig. 31. Shapes of 1.5, 1.8, 2.0, 2.5, 3.0, 3.5 and 4.0 mm Samples After Separation Test

6. Conclusions

The present study has been developed the interpretation processor including the behavior of material failure and the separation phenomena under transient dynamic loading (the operation of explosive bolt) using AUTODYN V4.3, SoildWork 2003 and TrueGrid V2.1 programs. The results from the present work are as follows;

1. Making model of shape, finite element, boundary conditions, material, and failure of the ridge-cut explosive bolt in the present study is solved easily using AUTODYN program.

2. Because TrueGrid generates a mesh by the powerful projecting a block mesh of our choice of refinement onto complex geometry, the complex boundary condition like the ridge-cut explosive bolt can be easily implemented in AUTODYN including pre-processor.

3. It has been demonstrated that the interpretation in the ridge-cut explosive bolt under dynamic loading condition should be necessary to the appropriate failure model and the basic stress of bolt failure is the principal stress. The principal stress of 17-4PH, failure stress, calculated the present interpretation is two times of static tensile stress, 2.8~3.0 E6 kPa, and the value of the principal stress is quietly correlated to the result from the actual experimental work and some different design (shape and amount of explosive) of explosive bolt.

4. The use of the interpretation processor developing the present work could be extensively helped to design the shape and the amount of explosives in the explosive bolt having a complex geometry.

5. It is also proved that the interpretation processor approach is an accurate and effective analysis technique. Applying the present interpretation processor, it could be able to make the design of several kinds of explosive bolt without actual production, to reduce especially the developing time and money.

7. References

1) Brauer, K. O.: *Handbook of Pyrotechnics*, Chemical Publishing Co. Inc., NY, 1974, pp 119-128.
2) Cole, J. K. and Wolfe, W. P.: ASP Base Plate Design and Explosive Bolt Test, Sandia Report, SAND 88-2543, 1988.
3) Lee, Y. J.: The Study of Development of Ridge-Cut Explosive Bolt (I), ADD Report, TEDC-421-000939, 2000, pp. 1-63.
4) Lee, Y. J.: The Study of Development of Ridge-Cut Explosive Bolt (II), ADD Report, TEDC-421-010649, 2001, pp. 1-72.
5) Meyer, M. A. and Murr, L. E.: *Shock Wave and High-Strain-Rate Phenomena in Metals*, Plenim Press, NY, 1981, pp. 51-63.
6) Poncelet, E. F.: Theory of Ridge-Cut, Stanford Research Institute Report 006-54, 1954, pp. 1-12.